



The Intrinsic Electronic Transport Properties of Germanene by Ensemble Monte Carlo Simulation

Meryem Derya Alyörük^{1,a,*}

¹Department of Physics, Faculty of Arts and Sciences, Aksaray University, 68100 Aksaray, Türkiye.

*Corresponding author e-mail address: mderyaozdemir@aksaray.edu.tr

Research Article

History

Received: 28.11.2025

Accepted: 10.04.2026



This article is licensed under a Creative Commons Attribution-NonCommercial 4.0 International License (CC BY-NC 4.0)

ABSTRACT

Using the Ensemble Monte Carlo (EMC) simulation technique, the electronic transport performance of germanene sheets is explored, where only intrinsic scattering effects are included. The transport properties of the material are obtained where intra- and inter-valley scatterings are considered. The average velocity of carriers as a function of time, the steady state velocity of carriers as a function of applied field curves, and the best linear fits to these curves at low fields at each temperature are made, and the mobility is calculated from the slope of these best lines. The evaluated velocity–electric field characteristics reveal a negative differential resistance (NDR) behavior. Carrier mobility as a function of temperature is obtained, exhibiting consistency with previously reported theoretical findings.

Keywords: Ensemble Monte Carlo, Germanene, Mobility, Scattering, Transport.

^a 0000-0002-7495-8014

1. Introduction

The isolation of monolayer graphene in 2004 marked a turning point in condensed matter physics [1], leading to the discovery of a wide class of two-dimensional (2D) materials with extraordinary physical and electronic properties. Graphene's planar honeycomb structure and its linear energy dispersion at the Fermi level give rise to charge carriers that behave as massless Dirac fermions and lead to ultrahigh carrier mobility. However, the absence of a bandgap restricts graphene's use in conventional semiconductor devices.

This limitation has motivated intense research into other elemental analogues of graphene—particularly silicon- and germanium-based 2D materials—collectively known as silicene and germanene. Theoretical predictions first suggested that these group-IV monolayers could adopt a low-buckled honeycomb geometry, which is energetically more favorable than the planar configuration [2, 3]. In this structure, the two sublattices are vertically displaced due to partial sp^2 – sp^3 hybridization, which introduces a controllable buckling height. Despite this geometric distortion, the band structure of silicene and germanene preserves linear π and π^* crossings at the K and K' points of the Brillouin zone, maintaining the Dirac-like behavior of charge carriers [3]. The buckled geometry not only breaks inversion symmetry but also enables bandgap modulation under an external electric field, a key feature for field-effect transistor applications [4].

Germanene, the germanium counterpart of graphene, was theoretically predicted to be stable as a free-standing

monolayer in 2009 [2,3]. Experimental realization followed in 2014, when D'ávila et al. successfully synthesized germanene via dry epitaxial growth on Au(111) surfaces, confirming its low-buckled hexagonal arrangement [5]. Since then, germanene has been fabricated on various metallic substrates such as Pt(111), Al(111) [6, 7], and Ge₂Pt [8], and even on semiconducting surfaces like MoS₂ [9, 10], which enable partial decoupling of the germanene electronic states from substrate interactions.

From a theoretical perspective, germanene combines the desirable characteristics of graphene with some unique advantages. The larger atomic radius of Ge leads to a more pronounced buckling ($\Delta \sim 0.64 \text{ \AA}$) [11,12,13] and a stronger spin–orbit coupling (SOC), which opens a finite bandgap ($\sim 24 \text{ meV}$) at the Dirac points [14, 15]. Moreover, due to its larger buckling, germanene exhibits high carrier mobility [16, 17, 19-22] and a tunable band structure [23,24], making it a promising material for spintronic and nanoelectronic applications.

Although free-standing germanene has not yet been fabricated, substrate-supported layers exhibit electronic and optical properties comparable to the FS (Free Standing) structure [25]. High SOC, pronounced buckling, and small effective mass make germanene more promising for practical applications than graphene or silicene [4,17,18]. Its high carrier mobility and easily tunable characteristics further strengthen its potential in nanoelectronics. Moreover, many unconventional properties of germanene remain unexplored, offering

new directions for both theoretical and experimental research.

The main objective of this study, among others, is to present a systematic investigation of the transport properties and, in particular, the mobility of monolayer germanene sheets as a function of temperature using an ensemble Monte Carlo method. We find that mobility decreases from about 13300 cm²/V.s, at 50 K to about 3900 cm²/V.s, at 300 K. Our mobility results are in agreement with available studies [19, 20], and we found that the mobility of germanene is greater than the mobility values of silicene for all temperatures considered in this study [27, 29, 30, 32].

2. Materials and Methods

In two-dimensional germanene, the buckled lattice geometry breaks the inherent crystal symmetry, thereby introducing unique properties that strongly affect electron scattering processes. In Ref. [2], the energy band structure and the stability of low buckled silicene and germanene sheets are studied. The analysis in Ref. [27] encompasses both the electronic band structure and the phonon scattering rates, incorporating contributions from LO/TO and LA/TA phonons, along with ZO and ZA out-of-plane modes associated with the buckling of silicene. Their findings indicate that the electrons couple not only with two-dimensional phonons but also strongly with the out-of-plane ZA phonons. A thorough investigation of the broken horizontal symmetry, similar to that found in silicene and germanene, is presented in Ref. [28], where the authors show that scattering processes involving ZA phonons display low-energy divergence.

The intrinsic electronic scattering mechanisms incorporated in this work comprise acoustic (LA, TA, ZA) and nonpolar optical (LO, TO, ZO) phonons. The evaluation of electronic transport in germanene sheets via ensemble Monte Carlo simulations necessitates the accurate determination of phonon scattering rates. For each scattering channel, the essential input parameters—namely the energy band structure, deformation potential constants, and sound velocities—are adopted from Ref. [27], where these quantities were extracted from first-principles calculations for use in analytical transport models. Owing to a factor-of-two discrepancy in the definition of acoustic scattering matrix elements between the present formulation (Eq. 1) and that of Ref. [27], the acoustic deformation potential constants reported therein are scaled by one-half in this study.

Furthermore, in Ref. [27], the out-of-plane acoustic (ZA) phonon dispersion, which exhibits a quadratic

dependence near the Γ point ($q \sim 0$), is approximated by a linear relation beyond a characteristic wavevector ($q > q_0$). As demonstrated in Ref. [28], the quadratic nature of the ZA mode at long wavelengths leads to a divergence in the electron–phonon scattering rate at low carrier energies. This divergence is neglected in Ref. [27], and for consistency, the present work adopts the same linearized approximation for ZA phonons, utilizing the corresponding deformation potential constant provided in that reference. Additionally, based on the same reference, the deformation potential constants were also used with an approximate value for germanene.

The carrier scattering by acoustic phonons (LA, TA, ZA) [33, 34] is treated as an elastic process and expressed as follows:

$$W(E_k) = \frac{2D_a^2 k_B T}{\sigma v_s^2 \hbar^3 v_F^2} E_k \quad (1)$$

here, E_k denotes the electron energy, expressed as $E_k = \hbar v_F |\mathbf{k}|$ where v_F is the Fermi velocity, taken to be approximately 5.3×10^7 cm/s for intrinsic germanene [11, 20]. D_a denotes the deformation potential constant corresponding to the specific scattering mechanism (LA, TA, or ZA phonons). Here, σ represents the surface mass density of the germanene sheet (5.76×10^{-8} g/cm²), v_s is the sound velocity associated with the respective phonon mode, k_B is the Boltzmann constant, and T stands for the absolute temperature. The material parameters employed in this study are summarized in Table 1.

Table 1. Approximated phonon-related parameters of germanene at the K point [11, 20].

Phonon mode	Phonon energy (meV)	Deformation potential	Sound Velocity (cm/s)
ZA	0	0.5 eV	5.3×10^4
TA	0	2.2 eV	3.12×10^5 [12]
LA	0	0.8 eV	5.32×10^5 [12]
ZO	20.0	6.0×10^7 eV/cm	
TO	35.0	0.9×10^8 eV/cm	
LO	35.0	1.0×10^8 eV/cm	

The second mechanism associated with lattice vibrations is the non-polar optical phonon (NPOP) scattering [26, 34]. In the simulations, optical phonon modes (LO, TO, ZO) are treated inelastically, and their scattering rates are given by

$$W(E_k) = \frac{D_0^2}{2\sigma\omega_0(\hbar v_F)^2} \{n_0(E_k + \hbar\omega_0) + (n_0 + 1)(E_k - \hbar\omega_0)\Theta(E_k - \hbar\omega_0)\} \quad (2)$$

here n_0 denotes the Bose–Einstein distribution function, and D_0 represents the deformation potential constant corresponding to the scattering mechanism under consideration. The plus and minus signs indicate phonon absorption and emission processes, respectively. ω_0 is the frequency of the optical phonons involved, and the Heaviside step function (Θ), ensures that a minimum energy of $\hbar\omega_0$ is required for phonon emission to occur. The approximated deformation potential constants and approximated optical phonon energies employed in this study are summarized in Table 1 and adopted from Ref. [20]. The sound velocities associated with the respective phonon modes are given in Table 1.

Ensemble Monte Carlo simulations [35, 36] involving 104 particles are performed by incorporating the aforementioned scattering mechanisms. The drift velocity of the carriers is evaluated using the semi-classical equations of motion, expressed as [26, 30, 31]:

$$v_d = v_F \frac{k_x}{|k|} \quad (3)$$

In this expression, k_x represents the wave vector component in the direction of the applied field. The time-dependent drift velocity, averaged over all particles, is calculated from (3), allowing the steady-state velocity to be determined for each field strength. Repeating this process for different fields yields the velocity–field relationship, from which the low-field mobility is obtained as the slope at low electric fields.

3. Results and Discussion

We investigate the electronic transport properties of monolayer germanene using an EMC technique, considering only the intrinsic scattering mechanisms discussed in Section 2. As noted above, since germanene and silicene possess comparable electronic dispersions, the studies of Li and colleagues[27] on silicene were used to approximate the band structure and optical phonon dispersion energies of germanene. Figure 1 further provides an example of phonon distributions, obtained from the study of Gaddemane[20].

We first present Figure 2, which shows the electron-scattering rates for the mechanisms included in this study as a function of electron energy for intrinsic germanene. The ZA, LA, and TA acoustic phonons provide the largest contributions, while optical phonon scattering remains weaker. The germanene material parameters are listed in Table 1, and Refs. [11, 20] report a Fermi velocity of 5.3×10^7 cm/s for intrinsic germanene.

To set the stage for the mobility analysis, we first examine how the saturation velocity of intrinsic germanene responds to the applied electric field. Figure 3 illustrates that, across all temperatures studied, the velocity initially rises to a maximum and

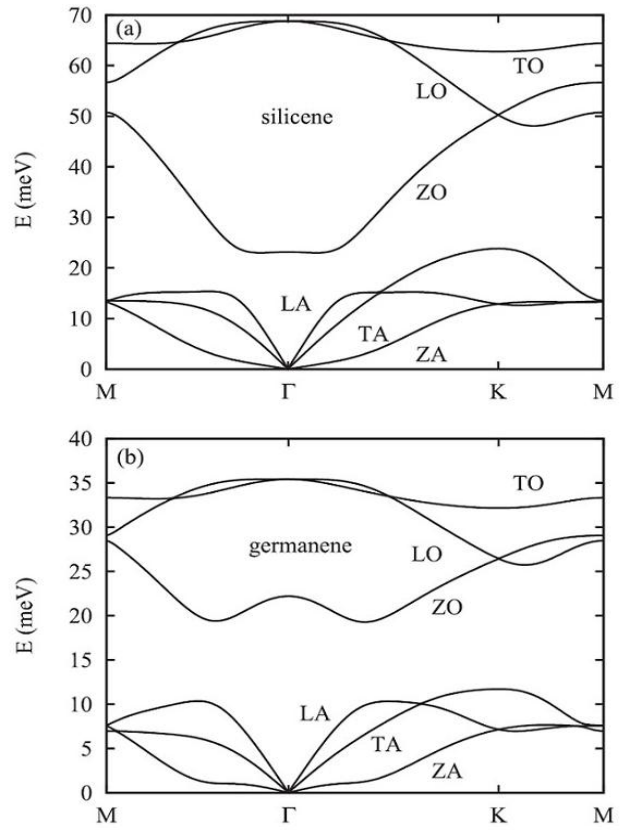


Figure 1. The phonon distribution of low buckled silicene (top) and germanene (bottom)[20].

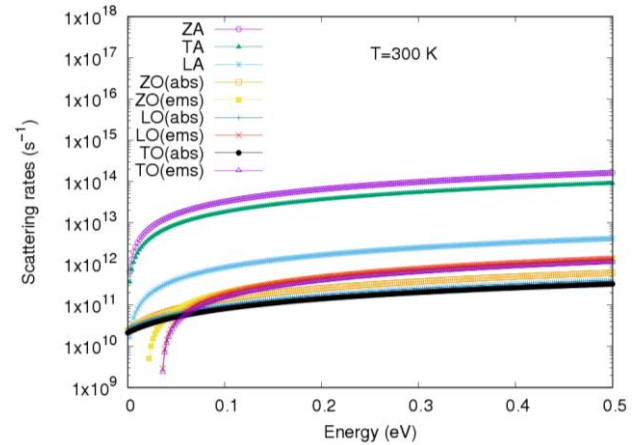


Figure 2. The electron scattering rates due to phonons for intrinsic germanene at $T = 300$ K, $v_F = 5.3 \times 10^7$ cm/s.

then decreases, demonstrating a negative differential resistance behavior. This NDR behavior is more significant than silicene, as mentioned in the study of Gaddemane et al.[20]. We have also observed the same behaviour in our previous study on silicene[32]. The outcomes of the aforementioned studies align well with the results of the present work. The field at which the peak occurs increases slightly with temperature. At 50 K, the peak velocity is about 7.2×10^6 cm/s at an applied field of approximately 0.8 kV/cm. The decline in velocity at higher fields is attributed to the increased electron energy, which enhances phonon scattering and thus reduces the saturation velocity.

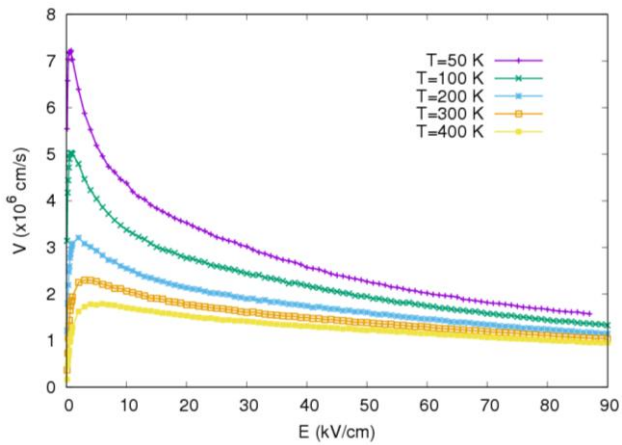


Figure 3. Steady state drift velocities as a function of applied field at various temperatures for intrinsic germanene, $v_F = 5.3 \times 10^7$ cm/s.

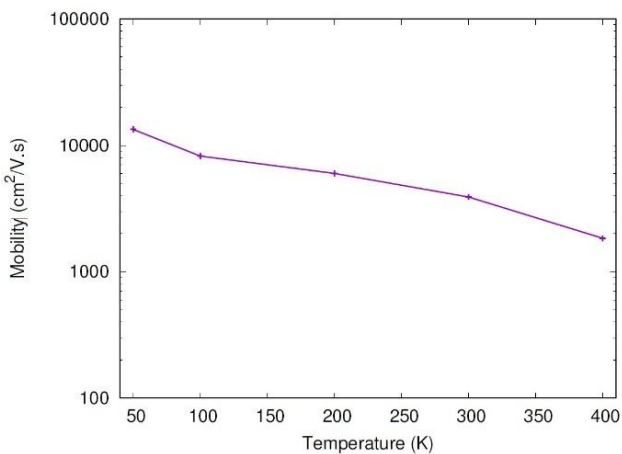


Figure 4. The variation of mobility with temperature for intrinsic germanene at low fields, $v_F = 5.3 \times 10^7$ cm/s.

As is evident from the literature, numerically estimated mobility values vary significantly, and there are currently no experimental measurements available for direct comparison. In this study, the mobility of germanene (Fig. 4) is obtained from the low-field regions of the velocity–field characteristics shown in Fig. 3. For each temperature, the best linear fit is extracted from its slope. The resulting intrinsic mobilities range from 13300 $\text{cm}^2/\text{V.s}$ at 50 K to 1840 $\text{cm}^2/\text{V.s}$ at 400 K, revealing a substantial variation with temperature. We have also checked the behavior of mobility as a function of temperature ($\mu = AT^{-\gamma}$), and found that $\gamma \approx 1.65$. The value of gamma ($\gamma \approx 1.65$) indicates that the mobility of monolayer germanene exhibits a strong temperature dependence, implying that charge transport is predominantly limited by intrinsic phonon scattering under ideal conditions [37].

4. Conclusion

The electron transport properties of a monolayer germanene sheet are investigated by an ensemble MC technique. Acoustic and nonpolar optic phonon scatterings are taken into account. The velocity decreases as the temperature increases, as expected, because acoustic phonon scattering increases linearly with

temperature. The carriers reach their peak velocity at low fields (1-6 kV/cm) and begin to decrease steadily. As the temperature increases, the peak velocities also decrease. The field at which the peak velocity is attained increases slightly as the temperature increases. The velocity-field curves of our study are compared with some of the existing results in the literature.

The mobility of carriers is calculated for monolayer germanene. The mobility decreases with temperature at a high rate. The NDR effect is observed for all cases and at all temperatures considered in this study for intrinsic germanene. The mobility values calculated for germanene are in the range of values provided in theoretical studies. In the study of Ni et al., the mobilities of suspended silicene and germanene, under an applied field of $E = 0.4 \text{ V}/\text{\AA}$ were estimated to be on the order of $10^5 \text{ cm}^2/\text{V.s}$ at room temperature [4]. Similarly, Ye et al. reported an intrinsic carrier mobility of approximately $6 \times 10^5 \text{ cm}^2/\text{V.s}$ for a monolayer germanene sheet, which exceeds even that of graphene [17,18,23]. In contrast, Gaddemane and co-workers obtained significantly lower room-temperature mobilities—3500 $\text{cm}^2/\text{V.s}$ in their 2017 study [19] and 2327 $\text{cm}^2/\text{V.s}$ in their 2018 work [20]—noting that these values are higher than the values reported for silicene.

Conflict of Interest

There are no conflicts of interest in this work.

Acknowledgments

The author declare that no funding or external support was received for this study.

References

- [1] Novoselov, K. S., Geim, A. K., Morozov, S. V., Jiang, D., Zhang, Y., Dubonos, S. V., Grigorieva, I. V., & Firsov, A. A. (2004). *Electric field effect in atomically thin carbon films*. *Science*, 306(5696), 666–669. <https://doi.org/10.1126/science.1102896>
- [2] Cahangirov, S., Topsakal, M., Aktürk, E., Şahin, H., & Ciraci, S. (2009). *Two- and one-dimensional honeycomb structures of silicon and germanium*. *Physical Review Letters*, 102(23), 236804. <https://doi.org/10.1103/PhysRevLett.102.236804>
- [3] Şahin, H., Cahangirov, S., Topsakal, M., Bekaroğlu, E., Aktürk, E., Senger, R. T., & Ciraci, S. (2009). *Monolayer honeycomb structures of group-IV elements and III–V binary compounds: First-principles calculations*. *Physical Review B*, 80, 155453. <https://doi.org/10.1103/PhysRevB.80.155453>
- [4] Ni, Z., Liu, Q., Tang, K., Zheng, J., Zhou, J., Qin, R., Gao, Z., Yu, D., & Lu, J. (2012). *Tunable bandgap in silicene and germanene*. *Nano Letters*, 12(1), 113–118. <https://doi.org/10.1021/nl203065e>
- [5] Dávila, M. E., Xian, L., Cahangirov, S., Rubio, A., & Le Lay, G. (2014). *Germanene: A novel two-dimensional germanium allotrope akin to graphene and silicene*. *New Journal of Physics*, 16, 095002. <https://doi.org/10.1088/1367-2630/16/9/095002>
- [6] Li, L., Lu, S-z., Pan, J., Qin, Z., Wang, Y-q., Wang, Y., Cao, G-y., Du, S., and Gao, H.-J. (2014). *Buckled Germanene Formation on Pt(111)*. *Advanced Materials*, 26, 4820–4824. <https://doi.org/10.1002/adma.201400909>

- [7] Derivaz, M., Dentel, D., Stephan, R., Hanf, M.-C., Mehdaoui, A., Sonnet, P., & Pirri, C. (2015). *Continuous germanene layer on Al(111)*. *Nano Letters*, 15, 2510–2516. <https://doi.org/10.1021/acs.nanolett.5b00085>
- [8] Bampoulis, P., Zhang, L., Safaei, A., van Gastel, R., Poelsema, B., & Zandvliet, H. J. W. (2014). *Germanene termination of Ge₂Pt crystals on Ge(110)*. *Journal of Physics: Condensed Matter*, 26, 442001. <https://doi.org/10.1088/0953-8984/26/44/442001>
- [9] Houssa, M., Scalise, E., van den Broek, B., Lu, A., Pourtois, G., Afanas'ev, V. V., & Stesmans, A. (2015). *Interaction of silicene and germanene with non-metallic substrates*. 574, 012015. <https://doi.org/10.1088/1742-6596/574/1/012015>
- [10] Zhang, L., Bampoulis, P., Rudenko, A. N., Yao, Q., van Houselt, A., Poelsema, B., Katsnelson, M. I., & Zandvliet, H. J. W. (2016). *Structural and electronic properties of germanene on MoS₂*. *Physical Review Letters*, 116, 256804. <https://doi.org/10.1103/PhysRevLett.116.256804>
- [11] Yan, J.-A., Stein, R., Schaefer, D. M., Wang, X.-Q., & Chou, M. Y. (2013). *Electron-phonon coupling in two-dimensional silicene and germanene*. *Physical Review B*, 88, 121403(R). <https://doi.org/10.1103/PhysRevB.88.121403>
- [12] Peng, B., Zhang, H., Shao, H., Xu, Y., Ni, G., Zhang, R., & Zhu, H. (2016). *Phonon transport properties of two-dimensional group-IV materials from ab initio calculations*. *Physical Review B*, 94, 245420. <https://doi.org/10.1103/PhysRevB.94.245420>
- [13] Chegel, R. & Behzad, S. (2020). *Tunable Electronic, Optical, and Thermal Properties of two-dimensional Germanene via an external electric field*. *Scientific Reports*, 10, 704. <https://doi.org/10.1038/s41598-019-57243-5>
- [14] Liu, C.-C., Jiang, H., & Yao, Y. (2011). *Low-energy effective Hamiltonian involving spin-orbit coupling in silicene and two-dimensional germanium and tin*. *Physical Review B*, 84, 195430. <https://doi.org/10.1103/PhysRevB.84.195430>
- [15] Shih, P.-H., Chiu, Y.-H., Wu, J.-Y., Shyu, F.-L., & Lin, M.-F. (2016). *Coulomb excitations of monolayer germanene*. *Scientific Reports*, 7, 40600. <https://doi.org/10.1038/srep40600>
- [16] Bianco, E., Butler, S., Jiang, S., Restrepo, O. D., Windl, W., & Goldberger, J. E. (2013). *Stability and exfoliation of germanene: A germanium graphene analogue*. *ACS Nano*, 7(5), 4414–4421. <https://doi.org/10.1021/nn4009406>
- [17] Ye, X.-S., Shao, Z.-G., Zhao, H., Yang, L., & Wang, C.-L. (2014). *Intrinsic carrier mobility of germanene is larger than graphene's: first-principle calculations*. *RSC Advances*, 4, 21216–21220. <https://doi.org/10.1039/C4RA01802H>
- [18] Acun, A., Zhang, L., Bampoulis, P., Farmanbar, M., van Houselt, A., Rudenko, A. N., Lingenfelder, M., Brocks, G., Poelsema, B., Katsnelson, M. I., & Zandvliet, H. J. W. (2015). *Germanene: The germanium analogue of graphene*. *Journal of Physics: Condensed Matter*, 27, 443002. <https://doi.org/10.1088/0953-8984/27/44/443002>
- [19] Gaddemane, G., Vandenbergh, W. G., & Fischetti, M. V. (2016). *Theoretical study of electron transport in silicene and germanene using full-band Monte Carlo simulations*. In *IEEE International Conference on Simulation of Semiconductor Processes and Devices (SISPAD)* (pp. 353–356). <https://doi.org/10.1109/SISPAD.2016.7605219>
- [20] Gaddemane, G., Vandenbergh, W. G., Van de Put, M. L., Chen, E., & Fischetti, M. V. (2018). *Monte-Carlo study of electronic transport in non-oh-symmetric two-dimensional materials: Silicene and germanene*. *Journal of Applied Physics*, 124, 044306. <https://doi.org/10.1063/1.5037581>
- [21] Muoi, D., Hieu, N. N., Nguyen, C. V., Hoi, B. D., Nguyen, H. V., Hien, N. D., Poklonski, N. A., Kubakaddi, S. S., & Phuc, H. V. (2020). *Magneto-optical absorption in silicene and germanene induced by electric and Zeeman fields*. *Physical Review B*, 101, 205408. <https://doi.org/10.1103/PhysRevB.101.205408>
- [22] Wu, Y., Hou, B., Chen, Y., Cao, J., Shao, H., Zhang, Y., Ma, C., Zhu, H., Zhang, R., & Zhang, H. (2021). *Strong electron-phonon coupling influences carrier transport and thermoelectric performances in group-IV/V elemental monolayers*. *npj Computational Materials*, 7, 145. <https://doi.org/10.1038/s41524-021-00619-0>
- [23] Behzad, S. (2018). *Effect of uni-axial and bi-axial strains and vertical electric field on free standing buckled germanene*. *Journal of Electron Spectroscopy and Related Phenomena*, 229, 13–19. <https://doi.org/10.1016/j.elspec.2018.09.003>
- [24] Rezania, H., Abdi, M., & Astinchap, B. (2025). *Local electronic interaction effects on electronic properties of tetragonal Germanene under bias voltage*. *Physica E: Low-Dimensional Systems and Nanostructures*, 165, 116098. <https://doi.org/10.1016/j.physe.2024.116098>
- [25] Chowdhury, S., Bandyopadhyay, A., Dhar, N., & Jana, D. (2017). *Optical and magnetic properties of free-standing silicene, germanene and T-graphene system*. *Physical Sciences Reviews*, 2(5), 23–70. <https://doi.org/10.1515/psr-2016-5102>
- [26] Shishir, R. S., & Ferry, D. K. (2009). *Velocity saturation in intrinsic graphene*. *Journal of Physics: Condensed Matter*, 21, 344201. <https://doi.org/10.1088/0953-8984/21/34/344201>
- [27] Li, X., Mullen, J. T., Jin, Z., Borysenko, K. M., Nardelli, M. B., & Kim, K. W. (2013). *Intrinsic electrical transport properties of monolayer silicene and MoS₂ from first principles*. *Physical Review B*, 87, 115418. <https://doi.org/10.1103/PhysRevB.87.115418>
- [28] Fischetti, M. V., & Vandenbergh, W. G. (2016). *Mermin-Wagner theorem, flexural modes, and degraded carrier mobility in two-dimensional crystals with broken horizontal mirror symmetry*. *Physical Review B*, 93, 155413. <https://doi.org/10.1103/PhysRevB.93.155413>
- [29] Yeoh, K. H., Ong, D. S., Ooi, C. H. R., Yong, T. K., & Lim, S. K. (2016). *Analytical band Monte Carlo analysis of electron transport in silicene*. *Semiconductor Science and Technology*, 31, 065012. <https://doi.org/10.1088/0268-1242/31/6/065012>
- [30] Borowik, P., Thobel, J.-L., & Adamowicz, L. (2016). *Monte Carlo study of electron transport in monolayer silicene*. *Semiconductor Science and Technology*, 31, 115004. <https://doi.org/10.1088/0268-1242/31/11/115004>
- [31] Ozdemir, M. D., Atasever, O., Ozdemir, B., Yasar, Z., & Ozdemir, M. (2016). *Transport Properties of Graphene and Suspended Graphene with EMC: The Role of Various Scattering Mechanisms*. *Journal of Electronic Materials*, 45, 4468–4475. <https://doi.org/10.1007/s11664-016-4708-4>
- [32] Ozdemir, M. D., Cekil, H. C., Atasever, O., Ozdemir, B., Yasar, Z., & Ozdemir, M. (2020). *Electron transport properties of silicene: Intrinsic and dirty cases with screening effects*. *Journal of Molecular Structure*, 1199, 126878. <https://doi.org/10.1016/j.molstruc.2019.126878>
- [33] Hwang, E. H., & Das Sarma, S. (2008). *Acoustic phonon scattering limited carrier mobility in two-dimensional extrinsic graphene*. *Physical Review B*, 77, 115449. <https://doi.org/10.1103/PhysRevB.77.115449>
- [34] Fang, T., Konar, A., Xing, H., & Jena, D. (2011). *High-field transport in two-dimensional graphene*. *Physical Review B*, 84, 125450. <https://doi.org/10.1103/PhysRevB.84.125450>
- [35] Tomizawa, K. (1993). *Numerical simulation of submicron semiconductor devices*. Artech House.
- [36] Jacoboni, C., & Lugli, P. (1989). *The Monte Carlo method for semiconductor device simulation*. Springer-Verlag.
- [37] Kaasbjerg, K., Thygesen, K. S., & Jacobsen, K. W. (2012). *Phonon-limited mobility in n-type single-layer MoS₂ from first principles*. *Physical Review B*, 85, 115317. <https://doi.org/10.1103/PhysRevB.85.115317>